Remote synchronization in star networks

A. Bergner,[1,3] M. Frasca,[2] G. Sciuto,[2] A. Buscarino,[2] E. J. Ngamga,[3] L. Fortuna,[2] and J. Kurths[3,4,5]
[1]*Institute of Physics, University of Potsdam, DE-14476 Potsdam, Germany*
[2]*DIEEI, Faculty of Engineering, University of Catania, IT-95125 Catania, Italy*
[3]*Potsdam Institute for Climate Impact Research (PIK), DE-14473 Potsdam, Germany*
[4]*Institute of Physics, Humboldt University, DE-12489 Berlin, Germany*
[5]*Institute for Complex Systems and Mathematical Biology, University of Aberdeen, Aberdeen AB24 3UE, United Kingdom*
(Received 12 April 2011; revised manuscript received 5 January 2012; published 15 February 2012)

We study phase synchronization in a network motif with a starlike structure in which the central node's (the hub's) frequency is strongly detuned against the other peripheral nodes. We find numerically and experimentally a regime of remote synchronization (RS), where the peripheral nodes form a phase synchronized cluster, while the hub remains free with its own dynamics and serves just as a transmitter for the other nodes. We explain the mechanism for this RS by the existence of a free amplitude and also show that systems with a fixed or constant amplitude, such as the classic Kuramoto phase oscillator, are not able to generate this phenomenon. Further, we derive an analytic expression which supports our explanation of the mechanism.

DOI: 10.1103/PhysRevE.85.026208 PACS number(s): 05.45.Xt, 89.75.Hc

I. INTRODUCTION

Networks of oscillatory units have been recently studied widely [1–4]. These kinds of systems serve as a modeling basis for a variety of systems from neuroscience [5], pattern recognition [6], chemistry [7], biology [8], climatology [9–11], ecology [12], social systems [13], or engineering as for instance in robot coordination [14], communication [15], and sensor networks [16], and as a general concept for understanding complex self-organizing systems. Gaining knowledge about networks of coupled dynamical systems helps in understanding several phenomena, in particular synchronization, self-organization, and information transfer in complex systems.

Many networks found in nature have a scale-free topology [1,17], which is a structure where just a few nodes—the so called hubs—hold the major bulk of the links. In this work we study a typical network motif of such a hub (Fig. 1). It is interesting to study synchronization in such a hub motif as it captures the essence of scale-free topologies.

Many articles on oscillatory networks focus on a rather homogenous distribution of the nodes' parameters across the network; that is, all nodes are either identical or just detuned within a small parameter range. This is very likely due to the possibility of an analytical treatment of the underlying equations, which becomes very complicated or even undoable if the network and thus the describing equations become too heterogenous. However, the assumption of homogeneity is, in fact, not fulfilled in most realistic situations, which means it is quite unlikely to find a real system made up of several absolutely identical subsystems.

Therefore, we study in this work an oscillatory network model and focus on a strong heterogeneity; precisely, the frequency of the hub is strongly detuned with respect to the peripheral nodes. We investigate phase synchronization (PS) in these motifs. Within this setup we focus on a phenomenon which we will call *remote synchronization* (RS), which is a situation in which two or more nodes, say n and m, which are not coupled directly, but through other nodes only, are phase synchronized, but (and this is important) the transmitter nodes, that is the nodes along the path from n to m, are not phase synchronized with n and m, respectively.

We also investigate RS experimentally. To this aim, we designed a complex network made of coupled electronic nonlinear oscillators and study it with respect to different values of the coupling strength. The experimental results obtained confirm the emergence of RS in real systems.

In addition to numerical and experimental studies, we give necessary conditions for the existence of RS and show that fixed amplitude systems, such as Kuramoto phase oscillators, cannot generate the phenomenon and explain this analytically as well.

The outline of this paper is the following. First we introduce our model and the parameters and give a description of the experimental setup. Then we describe the observed phenomena and present analysis of them. Finally, we discuss the outcome and explain the underlying mechanism.

II. MODEL AND EXPERIMENTAL SETUP

Since we want to focus on the mere phenomenon of synchronization, in particular PS, we chose a simple and paradigmatic model, namely the Stuart-Landau oscillator. This model is the most simple one having a harmonic limit cycle without any distortions, so we can exclude $n:m$ synchronization in our analysis for now.

We consider a network of diffusively coupled Stuart-Landau oscillators [7,18]. The equations are given by

$$\dot{u}_n = (\alpha + i\omega_n - |u_n|^2)u_n + \frac{\varkappa}{d_n^{\text{in}}}\sum_{m=1}^{N} g_{nm}(u_m - u_n), \quad (1)$$

where $u \in \mathbb{C}$, α is the (Hopf) bifurcation parameter which controls how fast the trajectory will decay onto the attractor, ω_n is the eigenfrequency of the individual uncoupled oscillator n, $\varkappa$ is the overall or global coupling strength, d_n^{in} is the in-degree of node n and is used to normalize the input into node n, and (g_{nm}) is the adjacency matrix, which is symmetric, since we consider bidirectional couplings.

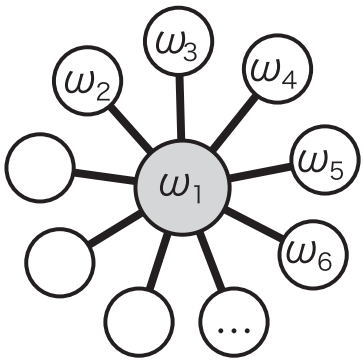

FIG. 1. Graphic visualization of a hub network motif (star motif).

Now we give the values of the parameters used for the simulations in this paper. The number of nodes has been set to $N = 5$ in correspondence with our experimental setup, but we also verified numerically the existence of the phenomenon for higher values of N. The decay parameter is $\alpha = 1$. As mentioned in the Introduction we are analyzing a hub motif (starlike network, Fig. 1), due to its importance as a building block for scale-free networks. Node 1 is chosen to be the hub and thus $n = 2,\ldots,N$ subscripts the peripheral nodes. The adjacency matrix is given by

$$(g_{nm}) = \begin{pmatrix} 0 & 1 & 1 & 1 & 1 \\ 1 & 0 & 0 & 0 & 0 \\ 1 & 0 & 0 & 0 & 0 \\ 1 & 0 & 0 & 0 & 0 \\ 1 & 0 & 0 & 0 & 0 \end{pmatrix}.$$

The in-degrees are $\{d_n^{\text{in}}\} = \{4,1,1,1,1\}$. We chose the frequency of the hub to be $\omega_1 = 2.5$ in the beginning, but we discuss the influence of a continuous change of this value later, as well. The peripheral nodes have a similar, but not identical, frequency since some repelling force is needed in order to see the transition to PS. The frequencies used in numerical simulations are $\{\omega_n\}_{n=2}^5 = \{0.975,0.992,1.008,1.025\}$

For the experimental realization Eq. (1) must be transformed into its equivalent real form which is given by

$$\frac{d}{dt}\begin{pmatrix} x_n \\ y_n \end{pmatrix} = \left[\begin{pmatrix} \alpha & -\omega_n \\ \omega_n & \alpha \end{pmatrix} - (x_n^2 + y_n^2)\mathbb{1}\right]\begin{pmatrix} x_n \\ y_n \end{pmatrix} + \frac{\varkappa}{d_n^{\text{in}}}\sum_{m=1}^{N} g_{nm}\left[\begin{pmatrix} x_m \\ y_m \end{pmatrix} - \begin{pmatrix} x_n \\ y_n \end{pmatrix}\right]. \quad (2)$$

The experimental setup is based on an electronic circuit mimicking the behavior of the Stuart-Landau oscillator. The circuit made of discrete components (operational amplifiers, multipliers realizing the nonlinearities of the oscillator, and a number of passive components such as resistors and capacitors) has been designed in order to obey to the same equations [Eq. (2)] of the Stuart-Landau oscillator, after appropriate scaling in frequency. We designed the circuit by following the guidelines reported in Ref. [19] and used, for instance, in Refs. [20,21]. The values of some components of the hub and peripheral circuits are chosen in a different way so that to realize the different simulation parameters used for hub and peripheral nodes. The circuits have been then coupled in such a way that a single resistor for each node controls the value of the coupling strength in Eq. (2). The circuit schematic, the governing equations, and the used component values are reported in the Appendix .

III. EMERGENCE OF REMOTE SYNCHRONIZATION

We start our analysis with a visual inspection of numerically integrated time series of system (1). Figure 2 depicts the excerpts from the time series, as well as the instantaneous frequencies and Lissajous-like patterns of the phases. For low coupling [Fig. 2(a)] we see that the nodes are interacting with each other and modulations of the phase appear, but no

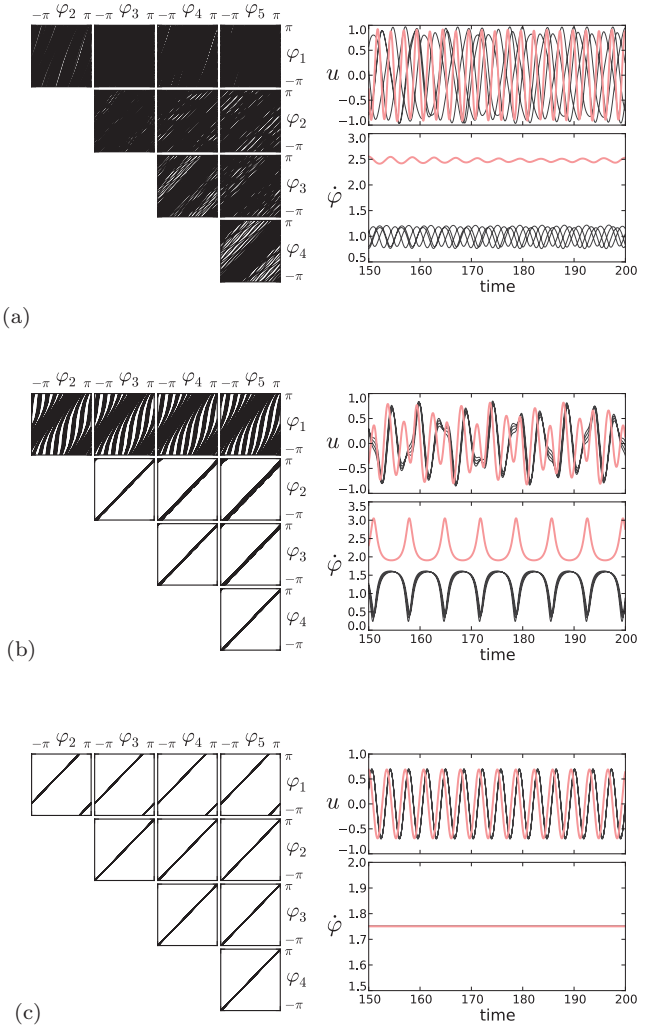

FIG. 2. (Color online) Plots to help in understanding the observed phenomena. For three different values of the coupling strength $\varkappa$ snapshots are shown of the time series $u(t)$, the instantaneous frequencies $\dot{\varphi}(t)$, and Lissajous-like figures made by plotting pairwise the phases φ_n of all oscillators against each other. The red (gray) line is the hub. (a) Snapshots for $\varkappa = 0.2$. Here no synchronization between any nodes is visible. (b) Snapshots for $\varkappa = 0.6$. Here we find RS. The peripheral nodes are synchronized with each other while the hub (node 1) remains unsynchronized with the rest. (c) Snapshots for $\varkappa = 0.8$. Regime of full PS. All nodes of the network are synchronized with each other.

synchronization is visible. For a strong coupling [Fig. 2(c)] we find a regime of full PS with an identical amplitude of all nodes and without any modulations. The phenomenon of RS appears for intermediate values of the coupling strength [Fig. 2(b)]. Here we see that all peripheral nodes become phase synchronized, while the hub remains with its own phase and frequency.

In order to study this more precisely, we introduce some measures for PS. The most common measure for PS is the Kuramoto order parameter, which is defined

$$r_{nm} = \left|\left\langle e^{i[\varphi_n(t)-\varphi_m(t)]}\right\rangle_t\right|, \tag{3}$$

where $\langle\cdot\rangle_t$ denotes the mean over time, and $\varphi_n(t)$ is the phase of oscillator n. For the Stuart-Landau oscillator the phase is simply given by $\varphi(t) = -i\,\ln(u/|u|)$.

Since we are interested in the situation where the peripheral nodes form one synchronized cluster and the hub is separated from this, that is, it forms another trivial cluster with itself, we introduce two measures accounting for that situation. For measuring the coherence of the hub with the rest of the network we define $r^{\text{direct}} = \frac{1}{N-1}\sum_{n=2}^{N} r_{1n}$. As a measure for the coherence of the peripheral cluster we define $r^{\text{indirect}} = \frac{2}{(N-1)(N-2)}\sum_{n=2,m>n}^{N} r_{nm}$, that is, the mean of the pairwise measured phase coherence among the peripheral nodes.

Figure 3 shows the transition to PS of both measures in dependence on the coupling strength $\varkappa$. The measures have been computed from numerical integration of Eq. (1) with the parameter setup given in Sec. II. Here it is clearly visible that the phase coherence of the peripheral nodes increases considerably faster than the synchronization of the hub with the rest. The peripheral nodes reach full PS at a value of the coupling strength $\varkappa$ of about 0.47, while the hub joins this cluster much later at $\varkappa \approx 0.74$, when it hits the global Arnold tongue of the network. In the figure we marked three steps in the curve of r^{indirect}. These steps correspond to the onset of RS between two, three, and all (four in our case) peripheral nodes of the network. These transitions are more clearly visible in Fig. 5(b) in which the number of synchronized clusters are

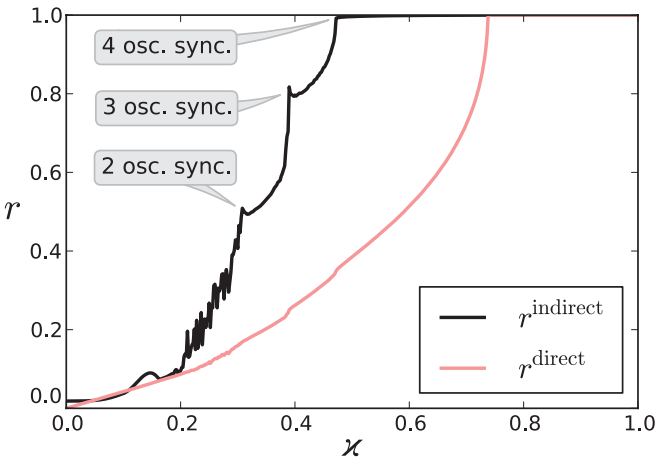

FIG. 3. (Color online) Transition to PS for the hub motif (Fig. 1). From the plot the onset of RS is clearly visible. The three annotations indicate synchronization between two, three, and four peripheral oscillators, respectively.

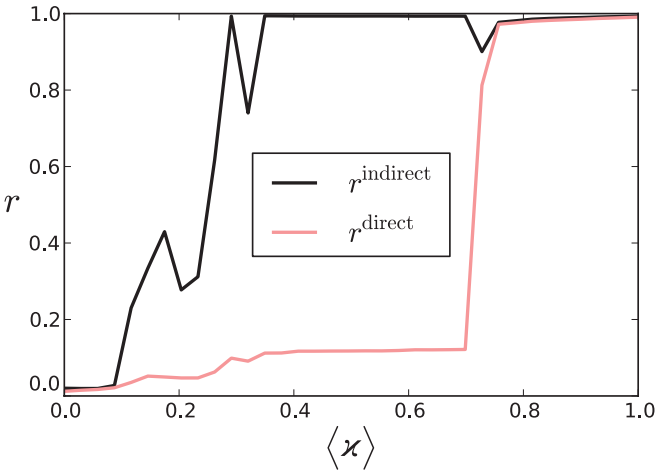

FIG. 4. (Color online) Transition to PS for the hub motif for experimentally obtained data. The regime of RS is clearly visible.

shown. This figure is discussed in more detail later in the article.

Figure 4 shows the same plot for experimentally generated data. The data have been obtained by a set of experiments on the implemented network of Stuart-Landau oscillator circuits performed with respect to different values of the coupling $\varkappa$, starting from $\varkappa = 1.0$ and decreasing this parameter. The coupling strength is decreased by small steps and for each value of it, the state variable x_n for each circuit has been acquired with a National Instruments USB6255 acquisition board with the sampling frequency $f_s = 300$ kHz. The phases of the oscillators have been then calculated by applying the Hilbert transform on the obtained time series and the two parameters r^{indirect} and r^{direct} have been calculated. The result, shown in Fig. 4, confirms the existence of RS in real systems. It should be noted that the coupling strength is implemented in the circuit through five different components, which makes it quite difficult to obtain exactly the same value for it, taking also into account the tolerances in the whole network circuit. For this reason, in Fig. 4 the average value $\langle\varkappa\rangle$ of this parameter is reported. The scenario observed is qualitatively similar to that obtained with numerical data, and the two transitions occur at slightly different values of the parameter. It is clearly visible that there exists a quite large domain of the coupling parameter, where we have RS while the hub remains with its own dynamics.

As a second analysis tool we are computing the Lyapunov spectrum (LS). Any nontrivial attractor (limit cycle, chaotic) of continuous dynamical systems has one Lyapunov exponent (LE) equal to zero, corresponding to the free phase of that system. Any perturbation in the direction of the system's flow will remain constant over time. In the case of an ensemble of uncoupled systems with a limit cycle or chaotic attractor, there will be as many zero LEs as there are systems included. As one couples those systems, PS will manifest itself by one or more (depending on the number of subsystems forming the synchronized cluster) LEs becoming strictly negative due to the attractive force between the former free phases of the oscillators [22]. Hence, the number of LEs equal to zero can be used as an indirect measure for the number of phase synchronized clusters.

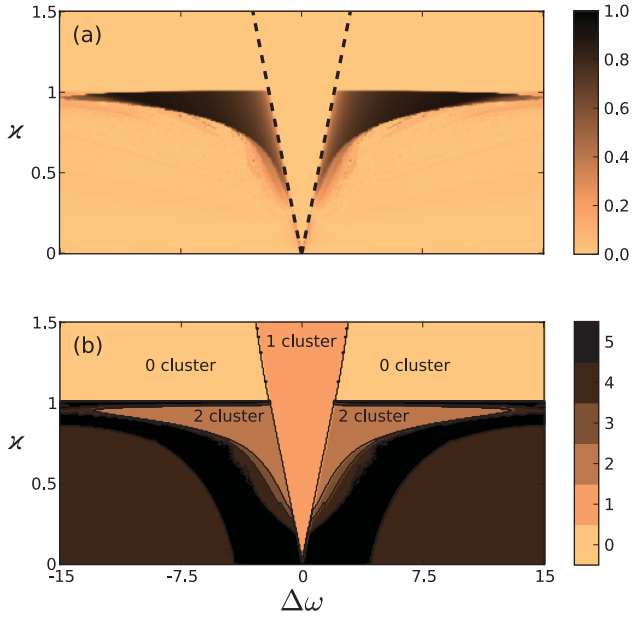

FIG. 5. (Color online) (a) Δr in dependence on $\Delta\omega$ and $\varkappa$, which can assume values between 0 and 1, whereby values close to 1 indicate RS (see text). The dotted line shows the analytically derived border of the Arnold tongue. The dark areas to the left and right of the Arnold tongue are regimes in which RS occurs. (b) The number of LEs equal to zero in dependence on $\Delta\omega$ and $\varkappa$. The two-cluster state corresponds to the RS regime.

In order to examine this phenomenon in more detail, we also studied the clustering in dependence on the hub's frequency. In Fig. 5(a) we plot $\Delta r := |r^{\text{direct}} - r^{\text{indirect}}|$ in dependence on the global coupling strength $\varkappa$ and the frequency mismatch $\Delta\omega$ of the hub with respect to the mean frequency of the peripheral nodes: $\Delta\omega := \omega_1 - \langle\omega_n\rangle_{n=2}^{N}$. In the case of RS r^{indirect} will be close to 1, while r^{direct} will be rather low, say less than 0.5, so Δr will be large here. If we are either in a regime where we have no synchronization or full synchronization r^{direct} and r^{indirect} will be about equal (either around 0 or around 1) and thus Δr will be low.

Figure 5(b) shows the number of LEs equal to zero for the same parameters $\Delta\omega$ and $\varkappa$. As already mentioned, this is an indirect measure for the number of synchronized clusters.

The dark area in Fig. 5(a) corresponds to the regime where RS exists. We find the same shape in Fig. 5(b) with a value of 2, thus showing that we have two synchronized clusters here. Both measures are in very good agreement with each other. For coupling strengths $\varkappa > 1$ and outside the Arnold tongue we have oscillation death, which manifests in the LS by all LEs becoming negative, since the system has only one global stable fixpoint. In both figures we clearly see the classical V-shaped Arnold tongue of the globally synchronized state, that is, a regime of one cluster PS.

For system (1), the Arnold tongue $\mathcal{A}$ can be computed analytically,

$$\mathcal{A} = \left\{\left(\varkappa, \{\omega_n\}_{n=1}^{N}\right) \mid \varkappa > \max_n |\Omega - \omega_n|\right\},$$

where Ω is the frequency inside the Arnold tongue, given by

$$\Omega = \frac{1}{2}\left(\omega_1 + \frac{1}{N-1}\sum_{n=2}^{N}\omega_n\right).$$

In Fig. 5(a) the analytically computed border of $\mathcal{A}$ is shown with dotted lines and agrees very well with the border observed from the numerically integrated data.

In the following we discuss the basic mechanism of RS and give an explanation for the necessary conditions for RS to occur robustly. We first describe the mechanism verbally and give a mathematical derivation afterward.

IV. MECHANISM UNDERLYING REMOTE SYNCHRONIZATION

Since we are interested in the mechanism of how two indirectly connected oscillators become synchronized, it is sufficient to focus on three nodes only: two peripheral nodes, to which we refer as nodes 2 and 3 (in correspondence with our initial numbering), connected indirectly via the hub (node 1). In order for nodes 2 and 3 to mutually synchronize, actions of node 2 need to be transmitted to node 3 and vice versa. It means that the dynamics of node 1 have to be such that they leave the transmitted actions of nodes 2 and 3 possibly unaltered. Thus, two conditions have to be fulfilled for RS to occur. First, the average time scale of the attractor of node 1 should be sufficiently different from the ones of the attractors of node 2 and node 3 in order to not to synchronize with them. Furthermore, nodes 2 and 3 must not be so different that they are able to synchronize through a weak interaction. Second, perturbations of node 1 must not decay too fast in order to get transmitted via node 1 .

The decay of perturbations of the Stuart-Landau oscillator is controlled by the parameter α in Eq. (1). The larger the α the faster a deviation from the limit cycle will "fall back" onto that. For $\alpha \to \infty$ any deviation of the amplitude will decay immediately. Thus, we expect that the RS regime disappears for $\alpha \to \infty$. In this case, after a change into polar coordinates and omitting the amplitude, Eq. (1) can be transformed into a network of coupled Kuramoto phase oscillators [7,23]:

$$\dot{\varphi}_n = \omega_n + \frac{\varkappa}{d_n^{\text{in}}}\sum_{m=1}^{N} g_{nm}\sin(\varphi_m - \varphi_n). \tag{4}$$

We applied the analysis described in Sec. III to this network of phase oscillators using the same setup and parameters as in the Stuart-Landau case described in Sec. II. Figure 6 shows $\Delta r(\Delta\omega, \varkappa)$ for this system. By comparing Fig. 6 with Fig. 5(a) the absence of the RS regime for the phase oscillators is clearly visible (absence of the dark areas to left and right of the Arnold tongue which indicate RS). We have also checked that by computing Δr for different increasing values of α. In this case the disappearance of the RS can be tracked. Thus, our previously made assumption, that the ability of indirectly coupled oscillators to synchronize remotely depends on a certain flexibility or memory of the amplitude of the transmitting system, is correct. Even more crucial is that it depends on the existence of a free amplitude at all. We show, in fact, that when amplitude perturbation is not possible, as for instance in coupled Kuramoto phase oscillators, for which a

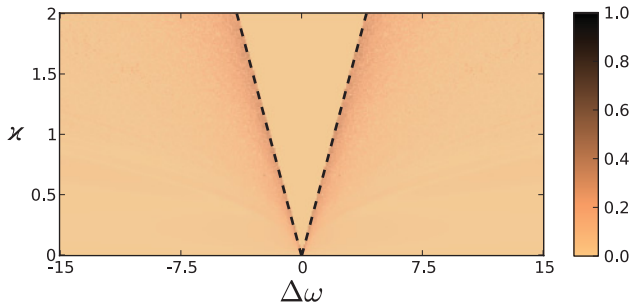

FIG. 6. (Color online) $\Delta r(\Delta\omega,\varkappa)$ for the hub motif of Kuramoto phase oscillators [Eq. (4)]. By comparing with Fig. 5(a) it can be observed that there is no RS regime here.

fixed not perturbable amplitude is assumed indirectly, RS does not appear.

Of interest is the dependence on the hub's frequency of the RS state, which cannot be explained with the above argumentation alone. In the following we derive some analytic description, which qualitatively accounts for that.

We come back to the situation of three coupled Stuart-Landau oscillators, as discussed in the beginning of this section. We linearize the hub oscillator around its limit cycle and leave the other two nodes untouched. We get the following equations:

$$\dot{u}_\mathrm{h} = (-2\alpha + i\omega_\mathrm{h})u_\mathrm{h} + \tfrac{1}{2}\varkappa(u_1 + u_2 - 2u_\mathrm{h}), \quad (5)$$

$$\dot{u}_{1,2} = (\alpha + i\omega_{1,2} - |u_{1,2}|^2)u_{1,2} + \varkappa(u_\mathrm{h} - u_{1,2}). \quad (6)$$

These equations describe two Stuart-Landau oscillators [Eq. (6)] coupled through a linear filter whose dynamics is described by the Eq. (5). Applying the Laplace transform we can write the transfer function for this filter:

$$H_\mathrm{h}(\omega) = \frac{\varkappa}{i\omega + 2\alpha + \varkappa - i\omega_\mathrm{h}}. \quad (7)$$

Using this, the hub can be replaced by an effective coupling coefficient, which is just a number derived from Eq. (7). Thus, we can write

$$\dot{u}_{1,2} = (\alpha + i\omega_{1,2} - \varkappa - |u_{1,2}|^2)u_{1,2} + \varkappa H_\mathrm{h}(\omega_{2,1})u_{2,1}. \quad (8)$$

From this perspective we are able to explain two main properties: First, obviously, since $\lim_{\alpha\to\infty} H_\mathrm{h} = 0$ the effective coupling strength between the two peripheral oscillators drops to zero and they are effectively uncoupled and, thus, unable to synchronize. This confirms our previous discussion of the mechanism as well as the numerically made analysis with Kuramoto phase oscillators. Second, by inspection of Eq. (7) the dependence of the coupling strength on the frequency of the hub is clear. The faster the hub oscillates the lower the effective coupling strength will be. Figure 7 shows the transition curve to RS in the $(\Delta\omega,\varkappa)$ plane for the discussed system of three oscillators in comparison with the system of two effectively coupled oscillators, as described by Eqs. (8) and (7). The simplified system can qualitatively describe the made observations and even agrees quantitatively for low and high values of the frequency mismatch $\Delta\omega$ adequately.

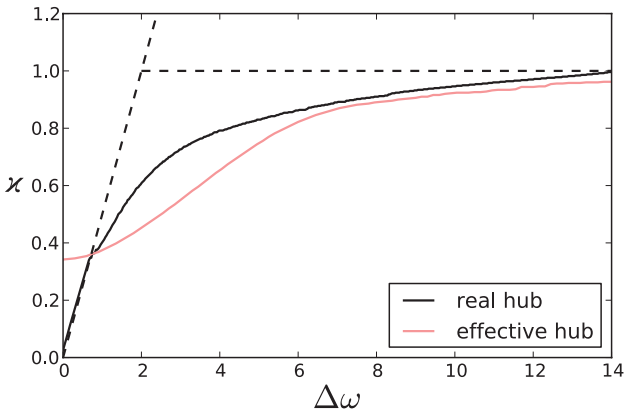

FIG. 7. (Color online) Comparison of the transition lines to RS between a system of three nodes (real hub), described by Eq. (1) with $N = 3$, and the linear approximation, described by Eqs. (8) and (7). The frequencies of nodes 1 and 2 are 0.975 and 1.025, respectively. The frequency of the hub has been changed from 1 to 15 (corresponds to $1 + \Delta\omega$). The dotted lines mark the regions of the Arnold tongue and of oscillation death and are inserted to help the reader by comparing with Fig. 5.

V. HIDDEN INFORMATION TRANSFER

Finally, we want to stress another important point. From our study we conclude that in the analysis of complex heterogeneous systems the choice of an appropriate correlation or information measure becomes more important. We demonstrate this with an example. Analogously to Eq. (3), we introduce another measure,

$$\rho_{nm} = \left|\left\langle e^{i[\theta_n(t)-\theta_m(t)]}\right\rangle_t\right|, \quad (9)$$

where $\theta(t) = \arctan[\mathcal{H}\ddot{\varphi}(t)/\ddot{\varphi}(t)]$ and $\mathcal{H}$ is the Hilbert transform operator (see the Appendix in Ref. [18] for details). We use the second derivative of φ in order to eliminate the bias. The measure ρ is an index for PS between the modulations of the instantaneous frequencies $\dot{\varphi}$, which are visible in Figs. 2(a) and 2(b). From visual inspection of those figures one sees that in the case of RS these modulations of $\dot{\varphi}$ are in synchrony among all nodes. Figure 8 shows for the same data which had

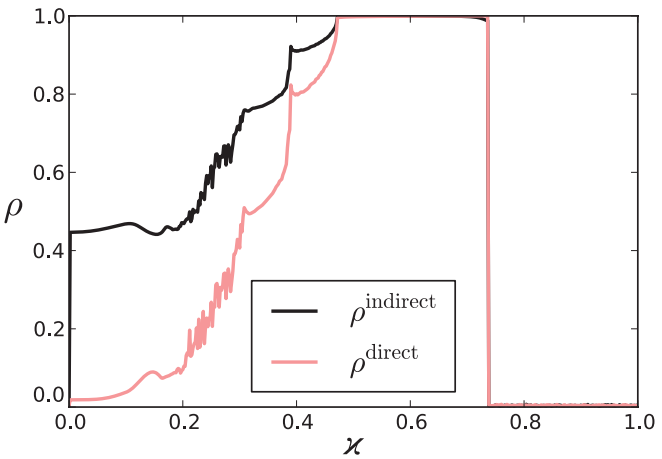

FIG. 8. (Color online) Transition of PS for the modulation of the instantaneous frequency of the nodes.

been used to create Fig. 3, the measures ρ^{direct} and ρ^{indirect} which are analogously computed to r^{direct} and r^{indirect} with r replaced with ρ. From the resulting graph one clearly sees that the phase modulations of all the oscillators in the network synchronize completely already at the first transition for $\varkappa \approx 0.47$. At $\varkappa \approx 0.74$ ρ drops to zero, which is due to the disappearance of the phase modulations (oscillation death due to a Hopf bifurcation; see Ref. [24]). With the measure ρ we are able to track the increase of the information transmission within the network. Other nonlinear phase space based measures (such as described in Ref. [25]) are also able to track this transition. In a more complex network, this or a similar method could be used to track the path through which certain remotely synchronized oscillators communicate. This is of special importance, in particular, related to the issue of inferring the network topologies from measured time series. Our example demonstrates that by using simple PS measures (as for instance r) the network's physical connectivity is obfuscated, but choosing other measures or—even better—combinations of different measures improved statements about the true connectivity of networks can be made.

VI. CONCLUSIONS

Our findings shed some new light on the issue of functional versus structural topology in networks of interacting dynamical systems, which is of high importance, especially in the field of neuroscience. We have shown that the measured topology via a "naive" PS measure gives a wrong picture of the underlying network structure and explained this by a mechanism, which we call RS. Nodes can "speak" with each other through a transmitting nodes without synchronizing with this one, given that the transmitter has a sufficiently different frequency.

We verified that RS also occurs in real experiments by designing a network of five coupled oscillators showing the regime of RS for coupling strength values which are intermediate between the case of no synchronization and that of PS of the whole network. Therefore, not purely phase oscillators may reveal phenomena that can be experimentally observed and that purely phase models are not able to explain.

Detailed analysis of RS has been carried out in the hub motif only, but preliminary studies in complex topologies show the occurrence of RS there as well. However, in such a scenario more complicated dynamics are possible and a detailed study with different analysis approaches has to be carried out.

RS might also find applications in several fields, such as neuroscience, in understanding information transmission inside the brain or in helping design new, more efficient artificial neural networks, as described in Ref. [6]. Another application might be in climate research, in particular in understanding teleconnections (i.e., long-range connections) such as between the Indian monsoon and El Niño-Southern Oscillation [10,11,26].

ACKNOWLEDGMENTS

This work was supported by DAAD/Ateneo Italo-Tedesco under the VIGONI Project, ECONS (WGL) and Volkswagen Foundation (Grant No. 85391).

APPENDIX: CIRCUIT

An assembly of coupled electronic circuits was used to test RS in real physical systems. In this Appendix, the electronic oscillator used and the coupling circuitry between the oscillators are briefly described.

The circuit that was built is governed by a rescaled version of Eqs. (2), that is, $\frac{d}{dt} \to \tau \frac{d}{dt}$, where τ is a time scaling factor ($\tau = 10^{-5} s$ in our circuit). The other circuit parameters were set to the values discussed in Sec. II. Figure 9 shows a schematic of the circuit. The values of the circuit components have been chosen in order to match Eqs. (2). In particular, the relationships between the parameters α and ω and the component values are given by

$$\alpha = \frac{R_6}{R_1} - 1 = \frac{R_{13}}{R_{10}} - 1, \quad \omega = \frac{R_6}{R_4} = \frac{R_{13}}{R_{11}}. \tag{A1}$$

Equations (A1) have been used to set the component values for the hub circuit and for the peripheral nodes. The

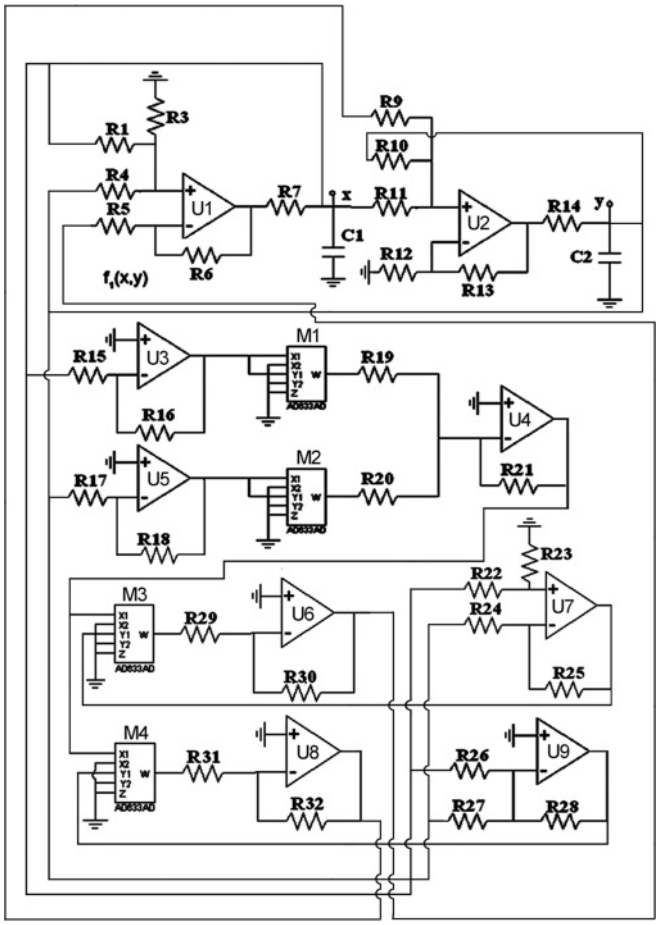

FIG. 9. Schematic of the circuit described by Eqs. (2) (rescaled in time with τ). The component values are $R_1 = 500\ \Omega$, $R_3 = R_4 = R_5 = R_6 = 1\ \text{k}\Omega$, $R_6 = 100\ \Omega$, $R_8 = R_9 = 4\ \text{k}\Omega$, $R_{10} = 2\ \text{k}\Omega$, $R_{11} = 4\ \text{k}\Omega$, $R_{12} = 1\ \text{k}\Omega$, $R_{13} = 4\ \text{k}\Omega$, $R_{14} = 100\ \Omega$, $R_{15} = 1\ \text{k}\Omega$, $R_{16} = 7.2\ \text{k}\Omega$, $R_{17} = 1\ \text{k}\Omega$, $R_{18} = 7.2\ k\Omega$, $R_{19} = R_{20} = R_{21} = R_{22} = 1\ \text{k}\Omega$, $R_{23} = R_{24} = 2\ \text{k}\Omega$, $R_{25} = 1\ \text{k}\Omega$, $R_{26} = 2\ \text{k}\Omega$, $R_{27} = R_{28} = R_{29} = R_{30} = R_{31} = R_{32} = 1\ \text{k}\Omega$, $C_1 = C_2 = 100\ \text{nF}$. The operational amplifiers $U1, \ldots, U9$ are all type TL084. The analog multipliers $M1, \ldots, M4$ are all type AD633. Power supply is ± 9 V.

component values listed in the caption of Fig. 9 refer to a peripheral node. The hub components differ from that of a peripheral node for the following resistors: $R_3 = 667\Omega$, $R_4 = 400\Omega$, $R_{11} = 1.6k\Omega$, $R_{12} = 727\Omega$. Resistors with 1% tolerances and capacitors with 5% tolerances have been used.

The experimental coupled oscillator setup consisted of five circuits arranged in a starlike network. The coupling terms $\varkappa(x_j - x_i)$ and $\varkappa(y_j - y_i)$ are produced by adding the x (respectively y) signals and multiplying them for a tunable gain factor through an operation amplifier in algebraic adder configuration. The tuning of the coupling coefficient is realized by using as feedback resistor a potentiometer. The coupling terms are then added into the equations of the electronic oscillator through the operational amplifier adders U1 [term $\varkappa(x_j - x_i)$] and U2 [term $\varkappa(y_j - y_i)$].

[1] S. Boccaletti, V. Latorab, Y. Morenod, M. Chavezf, and D.-U. Hwanga, Phys. Rep. **424**, 175 (2006).

[2] A. Arenas, A. Diaz-Guilera, J. Kurths, Y. Moreno, and C. Zhou, Phys. Rep. **469**, 93 (2008).

[3] G. V. Osipov, J. Kurths, and C. Zhou, *Synchronization in Oscillatory Networks* (Springer-Verlag, Berlin, 2007).

[4] S. Gil and A. S. Mikhailov, Phys. Rev. E **79**, 026219 (2009).

[5] E. M. Izhikevich, *Dynamical Systems in Neuroscience: The Geometry of Excitability and Bursting* (MIT Press, Cambridge, MA, 2006).

[6] M. Grant and K. R. Elder, Phys. Rev. Lett. **82**, 14 (1999).

[7] Y. Kuramoto, *Chemical Oscillations, Waves, and Turbulence* (Springer-Verlag, Berlin, Heidelberg, 1984).

[8] E. Ullner, A. Koseska, J. Kurths, E. Volkov, H. Kantz, and J. Garcia-Ojalvo, Phys. Rev. E **78**, 031904 (2008).

[9] J. F. Donges, Y. Zou, N. Marwan, and J. Kurths, Eur. Phys. J. Spec. Top. **174**, 157 (2009).

[10] J. F. Donges, Y. Zou, N. Marwan, and J. Kurths, Europhys. Lett. **87**, 48007 (2009).

[11] D. Maraun and J. Kurths, Geophys. Res. Lett. **32**, L15709 (2005).

[12] D. He and L. Stone, Proc. R. Soc. London B **270**, 1519 (2003).

[13] S. Gil and D. H. Zanette, Phys. Lett. A **356**, 89 (2006).

[14] A. Buscarino, C. Camerano, L. Fortuna, and M. Frasca, Phil. Trans. R. Soc. A **368**, 2179 (2010).

[15] A. Buscarino, L. Fortuna, and M. Frasca, Phys. Rev. E **75**, 016215 (2007).

[16] K. Konishi and H. Kokame, Chaos **18**, 033132 (2008).

[17] R. Albert and A.-L. Barabási, Rev. Mod. Phys. **74**, 47 (2002).

[18] A. Pikovsky, M. Rosenblum, and J. Kurths, *Synchronization—A Universal Concept in Nonlinear Science* (Cambridge University Press, Cambridge, 2001).

[19] L. Fortuna, M. Frasca, and M. G. Xibilia, in *Chua's Circuit Implementations: Yesterday, Today and Tomorrow*, World Scientific Series on Nonlinear Science, Series A, Vol. 65 (World Scientific, Singapore, 2009).

[20] E. J. Ngamga, A. Buscarino, M. Frasca, L. Fortuna, A. Prasad, and J. Kurths, Chaos **18**, 013128 (2008).

[21] A. Buscarino, L. Fortuna, and M. Frasca, Physica D **238**, 1917 (2009).

[22] M. Rosenblum, A. Pikovsky, and J. Kurths, Phys. Rev. Lett. E **76**, 1804 (1996).

[23] J. A. Acebrón, L. L. Bonilla, C. J. Prez Vicente, F. Ritort, and R. Spigler, Rev. Mod. Phys. **77**, 137 (2005).

[24] D. G. Aronson, G. B. Ermentrout, and N. Kopell, Physica D **41**, 403 (1990).

[25] T. Pereira, M. S. Baptista, and J. Kurths, Phys. Rev. E **75**, 026216 (2007).

[26] I. I. Mokhov, D. A. Smirnov, P. I. Nakonechny, S. S. Kozlenko, E. P. Seleznev, and J. Kurths, Geophys. Res. Lett. **38**, L00F04 (2011).